Neutron Irradiation of Alloy N and 316L Stainless Steel in Contact with a Molten Chloride Salt

N Dianne Bull Ezell[a], Stephen S. Raiman[b], J. Matt Kurley[c], Joel McDuffee[d]

[a] Oak Ridge National Lab 1 Bethel Valley Rd, Oak Ridge, TN 37830 United States bullnd@ornl.gov,
[b]raimanss@ornl.gov, [c]kurlyjm@ornl.gov, [d]mcduffeej@ornl.gov

Abstract—**Capsules containing NaCl-MgCl₂ salt with 316L stainless steel or alloy N samples were irradiated in the Ohio State University Research Reactor for 21 non-consecutive hours. A custom irradiation vessel was designed for this purpose, and details on its design and construction are given. Stainless steel samples that were irradiated during exposure had less corrosive attack than samples exposed to the same conditions without irradiation. Alloy N samples showed no significant effect of irradiation. This work shows a method for conducting in-reactor irradiation-corrosion experiments in static molten salts, and presents preliminary data showing that neutron irradiation may decelerate corrosion of alloys in molten chloride salts.**

Index Terms—**molten salt reactor, corrosion, irradiation, high-temperature experiment**

1. INTRODUCTION

Oak Ridge National Laboratory (ORNL) has been developing advanced measurement techniques and material studies in support of molten salt reactors since the 1960s when the Molten Salt Reactor Experiment (MSRE) was constructed and operated on site [1-6]. The molten salt coolant and fuel melts are known to be corrosive to salt-facing materials [7], and significant attention has been paid to understanding and quantifying corrosion in a variety of molten salt melts. One particularly challenging problem is studying the effect of radiation on corrosion of salt-facing materials. Irradiation may affect corrosion by several mechanisms. First, radiation enhanced diffusion may affect the diffusion of species to the salt-material interface [8]. This is especially important if diffusion of Cr is the rate-controlling mechanism, as asserted by Evans et al [9]. Second, radiation may create oxidizing or reducing species in the salt melt through radiolysis. Prior works have shown radiolytic production of fluorine [10] or chlorine [11] gas in low temperature solidified fluoride and chloride salt melts, respectively. Investigations during the MSRE concluded that radiolysis is not significant at operating temperatures [10], although this assertion was based on the lack of fluorine gas production from the melt, and the possibility exists that in-track radiolysis effects may affect material degradation. Lastly, electronic excitation of material surfaces may affect the rate of chemical reactions between the salt melt and the material. This effect has not been shown to affect corrosion in any condition, but Petri et al [12] have shown excess hydrogen production during irradiation of materials in water, and it stands to reason that it should at least be considered when irradiating materials exposed to molten salts.

Zhou et al. conducted experiments in which Ni-Cr alloys were exposed to FLiNaK salt while simultaneously irradiated with a proton beam, and found that irradiation decelerated corrosion of the alloy [13]. They attributed this deceleration to grain boundary self-healing due to the abundance of irradiation-produced interstitials in the irradiated alloy

This paper reports the method and results of an experiment in which molten salt capsules were exposed to neutron irradiation to study the effect of radiation on material corrosion. The design of

the experiment is detailed, along with characterization of samples showing the effect of neutron irradiation on corrosion in the chloride salt melt.

2. EXPERIMENT DESIGN: MATERIALS TESTED

For this work, two materials were tested: 316L stainless steel and alloy-N, often referenced as Hastelloy-N or INOR-8. The composition of the alloy heats from which samples were made is given in Table 1. Composition was measured using inductively coupled plasma mass spectroscopy (ICP-MS) and optical emission spectroscopy, inert gas fusion, and combustion analysis.

TABLE 1. Composition of the material heats used in this work

	Fe	Ni	Cr	Mo	Mg	Si	C	S	O	others
316H	64.5	13.3	17.2	2.3	1.9	0.54	0.058	0.016	0.008	Cu 0.08
Alloy N	3.7	71.9	7.2	16.0	0.27	0.26	0.052	0.0067	0.0011	Co 0.55

3. EXPERIMENT DESIGN: SALT PREPARATION

For this study, two eutectic melts of $NaCl$-$MgCl_2$ in a 58:42 molar ratio were prepared. The first , a "dry" melt, was prepared according to a process described more completely in previous works [14]. ACS grade $NaCl$ and 98% pure $MgCl_2$ were purchased from Alfa Aesar. The $NaCl$ was melted and sparged with CCl_4 for 3 hours, argon for 30 minutes, argon with 4% hydrogen for 1 hour, and argon again for 30 minutes. The $MgCl$ was purified by mixing it with NH_4Cl in a 2:1 $MgCl_2$:NH_4Cl ratio, and heating to 450°C, and held at that temperature for two hours before heating to 750°C, where it is held for one hour. The mixture was then sparged with CCl_4 at 850°C for 35-40 hours, followed by an argon sparge for 30 minutes. Following that, the mixture was sparged with argon-4% hydrogen for 12-15 hours, followed by another argon sparge for 30 minutes. Lastly, the $NaCl$ and $MgCl_2$ were mixed together in the desired 58:42 $NaCl$/$MgCl_2$ (molar) eutectic composition, heated to 850°C, and sparged with argon for 30 minutes. A "wet" melt was prepared by a "heat and cleave" method, a simpler method that involves no chemical purification and produces a more aggressive salt. The same ACS grade $NaCl$ and 98% pure $MgCl_2$ were fused together by heating to 800°C in an inert atmosphere, then cooled to a solid. The solid salt form was removed from the heating vessel, and a portion of the form was identified as having a higher oxide content due to its darker color. This portion was removed and discarded.

Acid-base titration was used to assess the oxide content of the salts after purification. The dry salt was measured at 29 ppm oxide, and the wet salt was found to have >1000 ppm oxide.

4. EXPERIMENT DESIGN: CAPSULE PREPARATION

The salt was loaded into molybdenum capsules, measuring 7.6 cm tall and 2.5 cm in diameter. Molybdenum was chosen due to its stability in molten salt [15] and its radiation tolerance [16]. The capsules were cleaned prior to use according to the steps in Table 2. Sample coupons measuring 13x6x1 mm were attached to the inside of an endcap of each capsule, one per capsule, as shown in Fig. 1. Then test specimens were fixed to the capsule lids with a thin wire. The capsule design is discussed in greater detail in a previous work [17].

TABLE 2. CLEANING PROCESS FOR MOLY CAPSULES

Cleaning Steps	Process
1	Mix 50 parts (by volume) acetic acid, 30 parts nitric acid, 5-10 parts hydrofluoric acid
2	Dip the Moly then gets dipped in this solution for about 5 seconds
3	After 5 second bath in the above mixture, the Moly is immediately dunked in concentrated HCl for another 10 seconds
4	After HCl, Moly gets washed with running water for about 30 to 60 seconds
5	Mo is then dried with blowing air
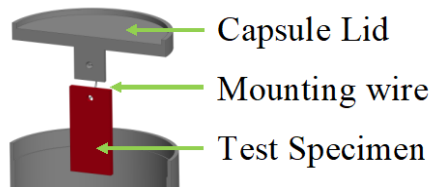
Fig. 1. Illustration of the mounting wire, test specimen, and capsule lid.

Each capsule was filled with 28g of solid salt in a glove box, and lids were press-fit onto the open end of the capsules. The capsules were transported in argon to an electron-beam welder where they were placed in the welder and pumped down to vacuum. During transport from the inert vessel, the outside surfaces of the capsules were exposed to air for <5 minutes. The capsule lids were press-fit and the capsules were full of heavier-than-air argon, so exposure of the salt to air was expected to be minimal. The welding chamber was pumped overnight before welding the lids shut.

A total of 6 capsules were used in this study, see Fig.2. Two capsules with stainless steel specimens and dry salt, two with stainless steel samples and wet salt, and two with alloy-N samples and wet salt. One capsule of each type was exposed with irradiation, and other was exposed without irradiation. Two capsules with alloy-N samples and dry salt were also prepared, but one cracked during welding so neither was used.
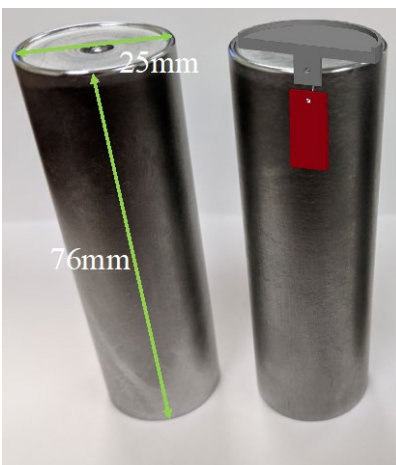
Fig. 2. Image of a fully assembled salt capsule.

5. IRRADIATION EXPERIMENT ASSEMBLY

The assembled molybdenum capsules were arranged in a stack of all the same orientation and wrapped in graphite foil, see Fig. 3. This was lowered into a Titanium primary containment. Before welding the primary containment closed, the entire assembly was vacuumed and back filled with Argon. The graphite foil inhibits capsule movement inside the primary containment. It is important to minimize unnecessary internal movements to reduce the chances of the mounting wire breaking.
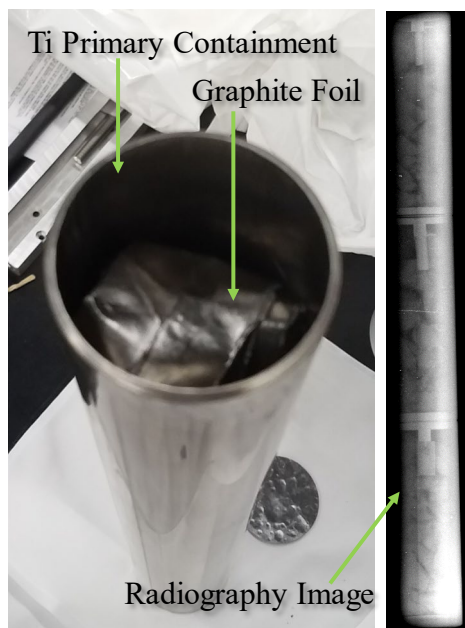
Fig. 3. Image of the primary containment housing the graphite foil wrapped salt capsules.

The sealed primary containment was then ready for shipping and irradiation. Recall, two complete experiments were fabricated simultaneously to expose the salt, test specimens, and assembly components to the same conditions through the assembly process. The irradiation was performed at the Ohio State Research Reactor (OSURR). This research reactor was selected because of its easy access to the pool top and the availability to 10" dry tube facility. Since the experiment required a tube shape furnace to bring the salt up to a molten temperature, it was

essential to find a large dry facility. A custom furnace by Thermcraft (maintaining 800 ºC at 600 Watts) was utilized for the duration of the irradiation. The furnace was designed to safely reach temperatures of 1100 ºC [16] and was powered using a Veeco 2500W DC linear power supply with a built-in controller. The temperature was regulated based off the temperature output of a thermocouple inside the furnace. A Ti basket was fabricated to support the furnace during loading and unloading. To monitor the experiment temperature, multiple thermocouples were tack welded at the top, middle, and bottom of the experiment. Also, several thermocouples monitored the internal temperature of the furnace (and control the power supply), the outer surface of the furnace and the ambient temperature above the furnace.

The experiment is loaded into the furnace manually and secured to ensure it does not fall and short out the heater wires inside the furnace. All of the electrical leads for power to the furnace and thermocouple extensions are connected to the lid of the secondary containment and tested. Then the furnace is lowered into the secondary containment and the lid is secured, see Fig. 4-5. The gas inlet is connected to a bottle of helium and the outlet was connected to an iCAM alpha beta air monitor. The system is purged several times through this system before pulled under vacuum, backfilled with Helium, and sealed for the irradiation.
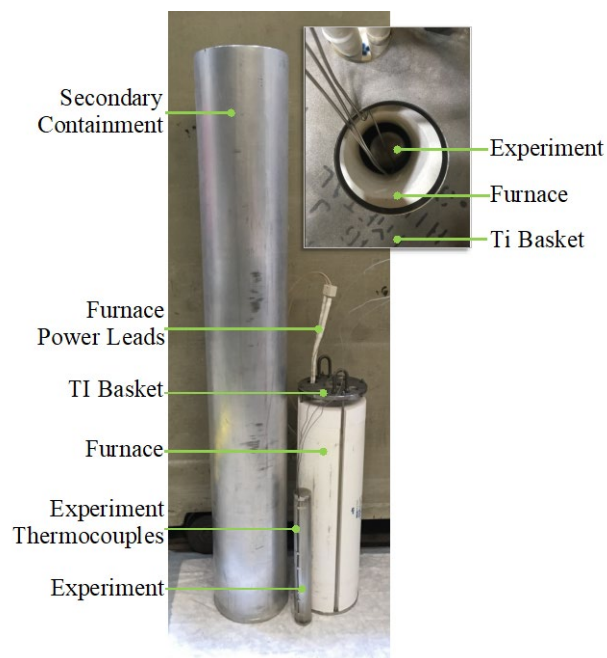

Fig. 4. Assembly at the Ohio State Research Reactor requires the experiment to be loaded into the furnace and then the furnace loaded into the secondary containment.
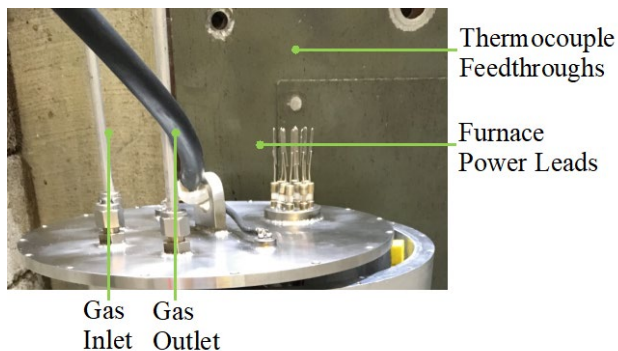
Fig. 5. Secondary containment lid with connections shown. This lid can be replaced with different feedthroughs as the irradiation experiments change.

A pully system with two points of contact was used to safely lower the fully assembled secondary containment into the 10" dry tube at the pool top of the reactor, see Fig. 6C. Once the experiment is resting at the bottom of the tube (Fig. 6A), the 10" dry tube is moved from the loading location to directly adjacent to the reactor core, see Fig. 6B. The dry tube will stay at this location for the duration of the irradiation.
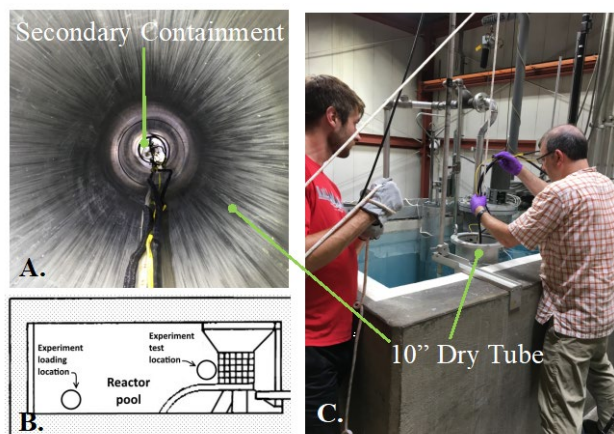

Fig. 6. A. An image of the secondary containment inside the 10" dry tube. B. A graphic of the reactor pool top. C. An image of the OSU team loading the experiment into the 10" dry tube.

6. IRRADIATION

The OSURR is a pool-type reactor licensed to operate at a maximum thermal power of 500kW and a maximum thermal neutron flux is approximately 1.7×10^{13} n/cm^2/s [18]. An irradiation was executed for a total of 21 hours, 7 hours per day across 3 days. As mentioned, the furnace maintained a temperature of 800 ºC after one hour of heating, see Fig. 7. For the 7 hours of heating, the reactor maintained 250 KW power with a thermal neutron flux of 10^{12} n/cm^2/s [19].
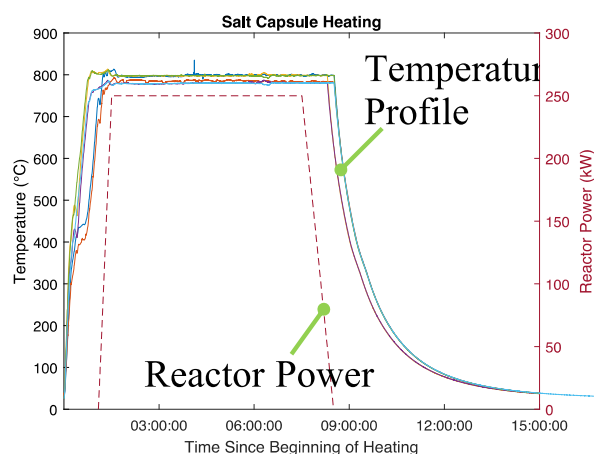
Fig. 7. Temperature and reactor power data from the irradiation experiment.

A neutron activation analysis was performed using and MCNP6 and SCALE 6.2 ORIGEN model of the OSURR reviewing the experiment (which included the capsules filled with salt inside the primary containment), furnace and cabling, and secondary containment [16]. The total expected dose rate of the primary containment and capsules at the end of the irradiation was 1.95 Rem/hr at 1m. However, the secondary containment with the furnace with cabling and the experiment was 1.74×10^3 Rem/hr at 1m. From these simulations, it was determined safe to handle the secondary containment five days after the irradiation was completed and safe to ship the experiment (Yellow II tag) 27 days later. The furnace and primary containment were stored at the OSURR for future irradiation experiments.

The temperature profile shown in Fig. 7 was replicated in the lab using identical infrastructure. The furnace and containment were developed to match those at the OSURR, see Fig. 8.
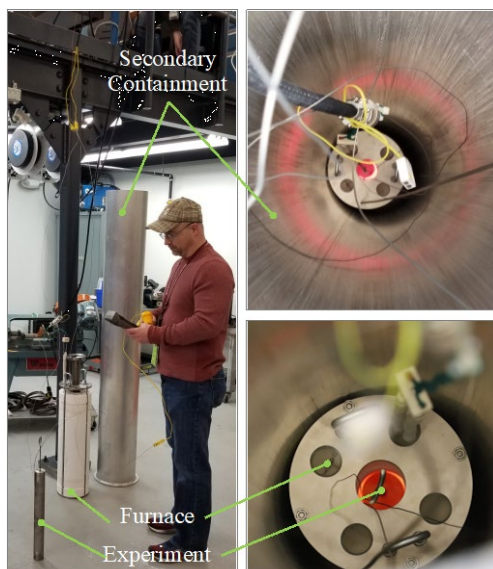

Fig. 8. Images from the out-of-pile experiment performed at ORNL.

7. POST IRRADIATION EXAMINATION

The primary containment was received at ORNL and transported to the Low Activation

Materials Development and Analysis (LAMDA) facility. LAMDA is a clean-room facility that provides the capability for microstructural characterizations, as well as, test thermal and mechanical properties at both room temperature and elevated temperatures [20]. The thermocouples were removed and disposed of as radiation waste. The first priority was to minimize the spread of removable contamination; therefore, all of the disassembly was performed in a glove box.

All of the PIE steps are performed on both the irradiated experiment as well as the out-of-pile experiment. The top of the primary containment was cut, and the capsules removed while still wrapped in the graphite foil. The foil and primary containment were surveyed enabling a comparison between the calculated activation analysis and the surveyed results and validates the mod/sim results. The bottoms of each of the capsules were then cut because the salt inside the capsules was solid around the test specimens (top end of the capsules), see Fig. 9. Due to the embrittlement of the Moly, the capsules were very easy to open. The larger pieces of the salt was chiseled away without damaging the specimen. The specimens are transferred to an ultrasonic bath removing the remaining salt, see Fig. 10 for clean specimen.
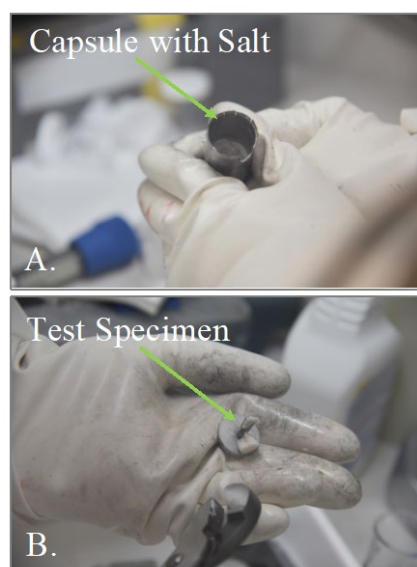

Fig. 9. Images from disassembly of the experiment in the LAMDA facility: A The open capsule with the bottom removed with the salt and specimen inside. B The test specimen attached to the top of the capsule before ultrasonic cleaning.

Fig. 10. Images of three of the cleaned test specimens.

The test specimens were removed from the top capsule lids, cross-sectioned, mounted in epoxy, polished, and imaged optically with a Leica MEF4A microscope. Samples were also characterized with scanning electron microscopy (SEM) and energy dispersive spectroscopy (EDS) on a Hitachi S-4800 equipped with EDAX hardware.

8. RESULTS

Representative optical micrographs of cross sectioned samples after exposure are shown in Fig. 11. The difference in color and sharpness of the micrographs is due to the use of different microscopes for inspecting irradiated and non-irradiated specimens. To quantify the depth of attack, 20 measurements were taken on optical micrographs of each sample, and the results are shown in Fig. 12.
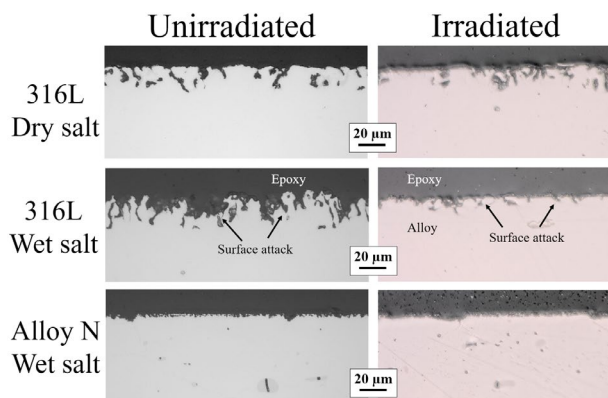

Fig. 11. Optical micrograph of 316L and alloy N samples after 21 hours of exposure to NaCl-MgCl$_2$ at 800°C with and without irradiation

The 316L samples exposed in dry salt show characteristic attack, with visible porosity near the exposed surface. The median depths of attack for the unirradiated and irradiated samples are 11 and 8 µm, respectively. More severe attack is visible on the 316L sample exposed in wet salt without irradiation, and the median depth of attack is 19 µm, which is much greater than the median depth of attack of 7 µm for the 316L samples exposed in wet salt with irradiation. The alloy-N samples both had much lower depth of attack, measuring 2 and 3 µm for the unirradiated and irradiated samples, respectively.
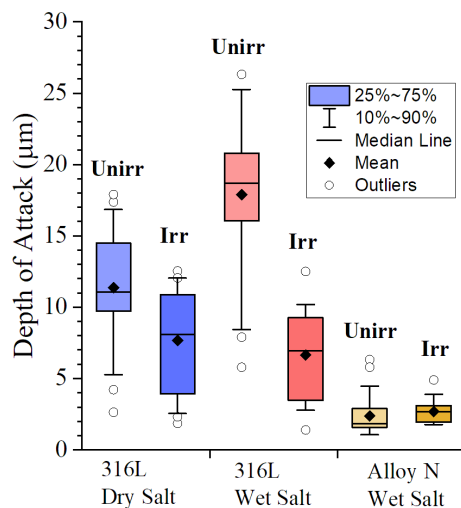
Fig. 12. Box and whisker plot showing depth of attack as measured on 316L and alloy N samples after 21 hours of exposure to NaCl-MgCl$_2$ at 800°C with and without irradiation.

Fig. 13 shows EDS micrographs of the samples after exposure. Chromium depletion near the surfaces is visible on the stainless steel samples, and less visible, though still present, on the alloy N samples. A distinct layer of Ni enrichment is also visible on the stainless steel samples in the regions where Cr is depleted. Similarly, a slight Mo enrichment is visible on the surface of the irradiated alloy N sample. It is not visible on the unirradiated sample, but this may be an artifact of the less-sensitive EDS detector on the SEM used for examination of the unirradiated samples.
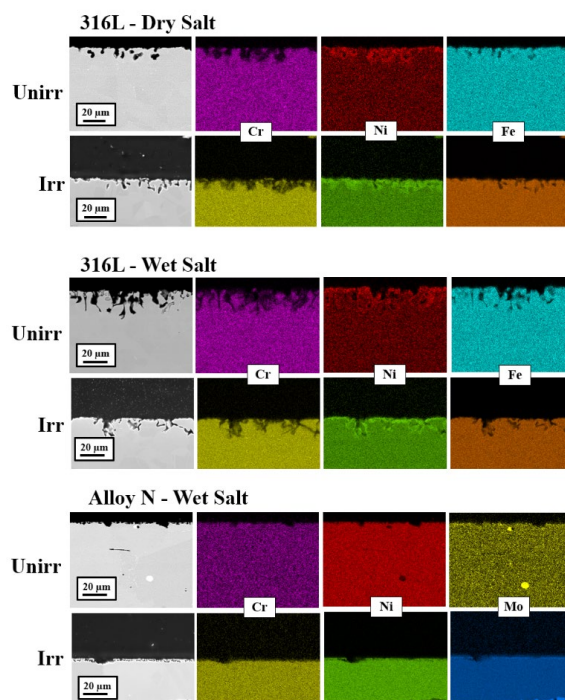

Fig. 13. EDS micrographs of 316L and alloy N samples after 21 hours of exposure to NaCl-MgCl$_2$ at 800°C with and without irradiation

9. Discussion

Figures 12 and 13 indicate that irradiation slowed corrosion of the stainless steel sample, and had little effect on the alloy-N sample. This is a compelling result, but for a few reasons, caution should be exercised before concluding that this effect is significant. First, the sample size in this work is small, and further corroboration is necessary. Molten salts are very hygroscopic, and corrosion rates are highly sensitive to salt purity [21], so larger data sets are necessary to convincingly attribute variations in corrosion rate to anything other than salt purity variation. For this work, all capsules were prepared together, and with the same batch of salt, to minimize variations. Still, unpredictable errors during handling still occur, and cannot be ruled out in this experiment. Second, while great effort was made to use the same temperature profile for the irradiated and unirradiated experiment (including using an identical irradiation vessel and heater for the unirradiated exposure), it remains a possibility that a variance in temperature profile accounts for the observed differences in corrosion.

With these caveats in mind, a few observations can be made. First, irradiation appears to have had a greater effect on the stainless steel sample exposed in wet salt. Comparing the unirradiated stainless steel samples in Fig. 13, the sample exposed in wet salt has a greater degree of attack, as expected, since wet salt is well known to be more aggressive [15, 21-23]. The sample irradiated in wet salt, however, has approximately the same degree of attack as the sample irradiated in dry salt. If this effect is real, it suggests a radiolysis effect in the salt that lessened the effect of oxidizing impurities. MSRE reports have suggested that salt radiolysis is not significant at operational temperatures in fluoride salt. However, those conclusions were reached based on the lack of fluorine gas production from the salt melt, and not on any corrosion results. Therefore, the possibility exists that in-track radiolysis effects may still occur. Further, radiolysis has been observed in molten chloride salt [24, 25], although it has not yet been linked to an increase or decrease in corrosion. If radiolysis of the salt is responsible for the decrease in stainless steel corrosion, the lack of an effect on corrosion of the alloy N sample remains unexplained.

Prior works have used a solid-state mechanism to explain irradiation decelerated corrosion. Hanbury et al [26]. found that irradiation enhanced diffusion of chromium led to the formation of a more protective oxide scale on stainless steel in 320°C water. This mechanism is not likely relevant to molten salt because a protective oxide scale does not form. The previously mentioned study by Zhou et al [13] attributed irradiation decelerated corrosion of a Ni-Cl alloy in FLiNaK salt to a solid-state mechanisms in which irradiation-produced interstitials aided the migration of Ni to grain boundaries, resulting in a "self-healing" effect. Again, if this mechanism was active in the present experiment, there is no explanation for why it is not active in alloy N, other than concluding that the total attack in the alloy N samples were too low to show any significant effects.

10. Conclusions and Future Irradiation Studies

Material interactions are a critical concern for the future of Molten Salt Reactors. Historically, Fluoride salts have been extensively studied but there are very few Chloride salt studies. ORNL demonstrated a first-of-its-kind irradiation experiment to study the effects of irradiation on corrosion development. This irradiation was performed at the Ohio State University Research Reactor

11. Acknowledgements

References

1. Delpech, S., et al., *Reactor physic and reprocessing scheme for innovative molten salt reactor system.* Journal of fluorine chemistry, 2009. **130**(1): p. 11-17.
2. Forsberg, C.W., P.F. Peterson, and R. Kochendarfer. *Design options for the advanced high-temperature reactor.* in *Proceedings of ICAPP.* 2008.
3. Forsberg, C.W., et al., *Liquid salt applications and molten salt reactors.* Revue Générale du Nucléaire, 2007. **4**: p. 63.
4. Ignatiev, V., et al., *Molten salt actinide recycler and transforming system without and with Th–U support: Fuel cycle flexibility and key material properties.* Annals of Nuclear Energy, 2014. **64**: p. 408-420.
5. Ignatiev, V. and A. Surenkov, *Corrosion phenomena induced by molten salts in Generation IV nuclear reactors*, in *Structural Materials for Generation IV Nuclear Reactors.* 2017, Elsevier. p. 153-189.
6. Serp, J., et al., *The molten salt reactor (MSR) in generation IV: overview and perspectives.* Progress in Nuclear Energy, 2014. **77**: p. 308-319.
7. Ergen, W., et al., *The Aircraft Reactor Experiment—Physics.* Nuclear Science and Engineering, 1957. **2**(6): p. 826-840.
8. Sizmann, R., *The effect of radiation upon diffusion in metals.* Journal of Nuclear Materials, 1978. **69**: p. 386-412.
9. III, R.B.E., J.H. DeVan, and G.M. Watson, *USAEC Report.* 1961, ORNL-2982, Oak Ridge National Lab., TN (USA).
10. Taboada, A., *Molten salt reactor program, Metallurgical developments.* 1964, ORNL-3708, Oak Ridge National Lab., TN (USA).
11. Tandon, L., *Radiolysis of Salts and Long-Term Storage Issues for Both Pure and Impure PuO2 Materials in Plutonium Storage Containers.* 2000, Report LA-13725-MS, Los Alamos National Laboratory.
12. Petrik, N.G., A.B. Alexandrov, and A.I. Vall, *Interfacial energy transfer during gamma radiolysis of water on the surface of ZrO2 and some other oxides.* The Journal of Physical Chemistry B, 2001. **105**(25): p. 5935-5944.
13. Zhou, W., et al., *Proton Irradiation-Decelerated Intergranular Corrosion of Ni-Cr Alloys in Molten Salt.* arXiv preprint arXiv:1911.11798, 2019.
14. Young, J. and G. Mamantov, *In-line sensors for electrolytic magnesium cells.* 1990, ORNL/M-13223, Oak Ridge National Lab., TN (USA).

15. Guo, S., et al., *Corrosion in the molten fluoride and chloride salts and materials development for nuclear applications.* Progress in Materials Science, 2018. **97**: p. 448-487.
16. Ezell, N., et al., *Examination of Corrosion Development in a Chloride Salt Irradiation Experiment*. 2019, Oak Ridge National Lab.(ORNL), Oak Ridge, TN (United States).
17. Raiman, S.S., et al., *Amorphous and partially-amorphous metal coatings for corrosion resistance in molten chloride salt.* Solar Energy Materials and Solar Cells, 2019. **201**: p. 110028.
18. Taylor, N.R., *Analysis of a High Temperature Fission Chamber Experiment for Next Generation Reactors*. 2017, The Ohio State University.
19. Ezell, N.D.B., et al., *Initial Irradiation Testing of Chloride Salts for Molten Salt Reactors.* Transactions, 2018. **119**(1): p. 451-453.
20. Nanstad, R.K., T. Yamamoto, and M. Sokolov, *Post-irradiation Examination Plan for ORNL and University of California Santa Barbara Assessment of UCSB ATR-2 Irradiation Experiment*. 2014, Oak Ridge National Lab.(ORNL), Oak Ridge, TN (United States).
21. Raiman, S.S. and S. Lee, *Aggregation and data analysis of corrosion studies in molten chloride and fluoride salts.* Journal of Nuclear Materials, 2018. **511**: p. 523-535.
22. Ouyang, F.-Y., et al., *Effect of moisture on corrosion of Ni-based alloys in molten alkali fluoride FLiNaK salt environments.* Journal of nuclear materials, 2013. **437**(1-3): p. 201-207.
23. Indacochea, J., et al., *High-temperature oxidation and corrosion of structural materials in molten chlorides.* Oxidation of metals, 2001. **55**(1-2): p. 1-16.
24. Pimblott, S.M., B.H. Milosavljevic, and J.A. LaVerne, *Radiolysis of aqueous solutions of 1, 1-and 1, 2-dichloroethane.* The Journal of Physical Chemistry A, 2005. **109**(45): p. 10294-10301.
25. LaVerne, J.A. and L. Tandon, *H2 and cl2 production in the radiolysis of calcium and magnesium chlorides and hydroxides.* The Journal of Physical Chemistry A, 2005. **109**(12): p. 2861-2865.
26. Hanbury, R.D. and G.S. Was, *Oxide growth and dissolution on 316L stainless steel during irradiation in high temperature water.* Corrosion Science, 2019. **157**: p. 305-311.